Biochemistry

 Volume 36, Number 5 February 4, 1997

Accelerated Publications

Structure of a Selectin-like Mutant of Mannose-Binding Protein Complexed with Sialylated and Sulfated Lewis^x Oligosaccharides[†,‡]

Kenneth K.-S. Ng and William I. Weis*

Department of Structural Biology, Stanford University School of Medicine, Stanford, California 94305

Received October 11, 1996; Revised Manuscript Received December 11, 1996[⊗]

ABSTRACT: Rat serum mannose-binding protein in which residues 211−213 have been changed to the Lys-Lys-Lys sequence found in E-selectin binds HL-60 cells and the oligosaccharide 3′-NeuAc-Le^x. To understand how this mutant, designated K3, mimics the carbohydrate-binding properties of E-selectin, structures of K3 alone and in complexes with 3′-NeuAc-Le^x, 3′-sulfo-Le^x, and 4′-sulfo-Le^x have been determined at 1.95−2.1 Å resolution by X-ray crystallography. The region of K3 that interacts with bound oligosaccharides superimposes closely with the corresponding region of unliganded E-selectin. In each of the oligosaccharide−protein complexes, the 2- and 3-OH of Fuc coordinate Ca^{2+} and form a network of cooperative hydrogen bonds with amino acid side chains that also coordinate the Ca^{2+}. Lys^{211} of the K3 mutant, which corresponds to Lys^{111} of E-selectin, interacts with each of the three bound ligands: the Nζ atom donates a hydrogen bond to the 4-OH of Gal in 3′-NeuAc-Le^x, forms a water-mediated hydrogen bond with the 4-OH of Gal in 3′-sulfo-Le^x, and forms a salt bridge with the sulfate group of 4′-sulfo-Le^x. Lys^{213} packs against an otherwise exposed aromatic residue and forms a water-mediated hydrogen bond with Lys^{211} which may help to position that residue for interactions with bound oligosaccharides. These structures are consistent with previous mutagenesis and chemical modification studies which demonstrate the importance of the Ca^{2+} ligands as well as Lys^{111} and Lys^{113} for carbohydrate binding in the selectins, and they provide a structural basis for understanding the selective recognition of negatively charged Le^x derivatives by the selectins.

Selectins are integral membrane proteins that mediate adhesion between leukocytes and endothelial cells during the transient rolling phase of leukocyte migration (McEver, 1994; Nelson et al., 1995). E- and P-selectin are expressed on activated endothelium, whereas L-selectin is constitutively expressed on neutrophils, monocytes, and most lymphocytes. Each selectin contains an NH_2-terminal C-type carbohydrate recognition domain (CRD)[1] connected to an epidermal growth factor-like domain and two to nine complement consensus repeats. Although physiological ligands have not been fully characterized, various lines of evidence indicate that the adhesion activity of the selectins is mediated primarily by the binding of O-linked oligosaccharides to the CRD. Oligosaccharides containing the Le^x structure (Galβ1−4[Fucα1−3]GlcNAc) derivatized at the 3-OH of Gal with either sulfate or NeuAc are some of the most effective natural

[†] This work is supported by Grant GM50565 from the National Institutes of Health. W.I.W. is a Pew Scholar in the Biomedical Sciences.

[‡] The coordinates and structure factors have been deposited in the Brookhaven Protein Data Bank (codes 1KMB, 2KMB, 3KMB, and 4KMB).

* To whom correspondence should be addressed.

[⊗] Abstract published in *Advance ACS Abstracts*, January 15, 1997.

[1] Abbreviations: CRD, carbohydrate recognition domain; Fuc, L-fucose; Gal, D-galactose; GlcNAc, *N*-acetyl-D-glucosamine; Le^a, Lewis^a; Le^x, Lewis^x; MBP, mannose-binding protein; MPD, 2-methyl-2,4-pentanediol; NeuAc, *N*-acetylneuraminic acid; PEG, polyethylene glycol; rmsd, root mean square deviation.

S0006-2960(96)02564-0 CCC: $14.00

small molecule ligands identified [reviewed in Varki (1994)].

The mode of oligosaccharide binding to the selectins is still poorly understood, even though the structure of a fragment of E-selectin containing the CRD and EGF domains has been determined to 2.0 Å resolution by X-ray crystallography (Graves et al., 1994). Current models of oligosaccharide binding in the selectins are derived from studies in which energy-minimized carbohydrate ligands have been docked into the unliganded E-selectin structure to satisfy electrostatic and steric constraints, nuclear Overhauser effect measurements, and inferences from site-directed mutagenesis and chemical modification studies (Cooke et al., 1994; Graves et al., 1994; Kogan et al., 1995; Scheffler et al., 1995). Unfortunately, these methods do not provide a precise structure of the bound oligosaccharide and its interactions with the protein.

Because it has not yet been possible to predict precisely or to determine directly the structures of ligands bound to the selectins, it has been necessary to adopt an indirect approach to study the mechanism of oligosaccharide binding. Rat serum mannose-binding protein (MBP-A) has provided a tractable experimental system for studying the determinants of carbohydrate binding in a wide variety of C-type lectins (Iobst & Drickamer, 1994, 1996; Iobst et al., 1994; Kolatkar & Weis, 1996). The K3 mutant of MBP-A, in which the sequence of residues 211−213 is changed to Lys-Lys-Lys, the corresponding sequence at positions 111−113 of E-selectin, gains the essential aspects of carbohydrate recognition by E-selectin, including binding to HL-60 cells and serum albumin derivatized with 3′-NeuAc-Le^x (Blanck et al., 1996).

Structures of a bacterially expressed form of K3 containing the CRD and the coiled-coil trimerization domain (Weis & Drickamer, 1994) have been determined for the unliganded protein, as well as for complexes with each of three different Le^x oligosaccharides derivatized with NeuAc and sulfate. The structure of the carbohydrate-binding site in K3 is remarkably similar to the corresponding region of unliganded E-selectin, suggesting that the K3-oligosaccharide complex structures reflect the mode of binding to selectins. These structures provide precise conformations of three bound oligosaccharides and suggest why the newly introduced Lys residues in K3 confer selectin-like binding specificity to MBP-A.

EXPERIMENTAL PROCEDURES

Materials. 3′-NeuAc-Le^x, 3′-sulfo-Le^x, and 4′-sulfo-Le^x were obtained from Toronto Research Chemicals.

Protein Purification. K3 was expressed in *Escherichia coli* and purified as described previously (Weis et al., 1991; Blanck et al., 1996). A proteolytic fragment was prepared by clostripain digestion, reverse-phase HPLC, and lyophilization prior to crystallization, as described (Weis & Drickamer, 1994).

Crystallization. Lyophilized K3 was dissolved in water at 5 mg/mL. The protein was neutralized with 50 mM NaOH, and $CaCl_2$ was added to a final concentration of 5 mM (final protein concentration of 2 mg/ml). Protein (2 μL) was mixed with 2 μL of solution A [8−10% (w:v) PEG 8000, 2% PEG 1000, 100 mM Tris-HCl (pH 7.8), 200 mM NaCl, 20 mM $CaCl_2$, and 2 mM NaN_3] to form a hanging drop, and the drop was equilibrated over 1 mL of solution A at 22 °C. Single crystals (approximately 80 μm × 50 μm × 20 μm) were harvested after 1 week and washed in solution A. Washed crystals were introduced as seeds into freshly prepared drops containing 2 μL of the above protein plus 2 μL of water plus 2 μL of solution A. Drops were equilibrated over 1 mL of solution A for 1−2 weeks before crystals were harvested (average size, 200 μm × 200 μm × 100 μm). Crystals of K3 are in the same space group, *C*2, as crystals of wild-type MBP-A, but the unit cell dimensions vary by up to 1 Å in different crystals (Table 2).

Crystal Soaking and X-ray Diffraction Measurements Crystals were adapted to solutions containing either MPD (unliganded and 3′-NeuAc-Le^x complex) or PEG 400 (3′- and 4′-sulfo-Le^x complexes) as cryosolvents. For adaptation to MPD, crystals were serially transferred to solutions containing solution A plus 5, 10, 15, and 20% MPD. For adaptation to PEG 400, crystals were serially transferred to solution A modified by varying the amount of PEG 8000 and PEG 400 present: 8% PEG 8000 + 4% PEG 400, 5% PEG 8000 + 10% PEG 400, 2% PEG 8000 + 15% PEG 400, and 30% PEG 400. Crystals were held in each solution for 15 min. In experiments where oligosaccharides were introduced, oligosaccharides were added to the last two solutions at 80−100 mM, which corresponds to a molar ratio of oligosaccharide:protein of >1000 for the K3 crystals used for data collection. [The equilibrium dissociation constant, K_d, is not known for any ligand binding to K3, but it is likely that the ligand concentrations used are at least $10K_d$, as the K_d of other MBP−oligosaccharide interactions falls in the 1−10 mM range (Iobst et al., 1994).] The final soak solutions were 5 μL hanging drops suspended over well solutions containing 1 mL of the mother liquor containing 80−100 mM sucrose in place of the oligosaccharide.

After adaptation to PEG 400 or MPD, crystals were suspended in a rayon loop and flash-cooled at ∼100 K. Data were measured on an R-AXIS IIC imaging plate detector (Rigaku) using Cu Kα radiation from a rotating anode (Rigaku; 50 kV, 90 mA, graphite monochromator, and 0.3 mm collimator) at a crystal-to-detector distance of 95 mm. Data for the 3′-sulfo-Le^x complex were measured at Stanford Synchrotron Research Laboratory beam line 7-1 using a Mar Research image plate detector (wavelength of 0.98 Å, crystal-to-detector distance of 140 mm). Lorentz polarization-corrected integrated intensities were obtained using DENZO (Otwinowski, 1993), and redundant measurements were scaled and merged with SCALEPACK. Each data set was put on a quasi-absolute scale using TRUNCATE of the CCP4 package (Collaborative Computational Project No. 4, 1994). Data processing statistics are presented in Table 1. X-PLOR was used for reciprocal space refinement and electron density map calculation (Brünger, 1992b); model building was performed using O (Jones et al., 1991), and the geometry of each model was monitored throughout refinement using X-PLOR and PROCHECK (Laskowski et al., 1993).

The starting model for refinement consisted of all protein atoms and ions in the MBP-A trimer structure (Weis & Drickamer, 1994) with the exception of residues 211−213, which were replaced by Ala. Before the start of refinement, a random set of reflections comprising 10% of all measured data was reserved as a test set for calculations of a free *R* factor, which was monitored throughout the course of refinement (Brünger, 1992a). For each structure, rigid-body minimization was used to place the model in the unit cell prior to repeated rounds of individual atom positional and

Table 1: Crystallographic Data[a]

crystal	intensity data: maximum resolution (Å)	independent reflections	completeness (%)	average redundancy	R_{sym}[b]	refinement: number[c] used [$F > 2\sigma(F)$]	R_{cryst}[d] (%)	R_{free}[e] (%)
K3	2.1	36 862	99.5 (99.0)	2.9 (2.7)	5.3 (27.6)	29 092	20.2	26.5
+3′-NeuAc-Le^x	2.0	41 761	98.6 (93.2)	2.4 (2.1)	6.0 (26.4)	35 319	19.0	24.7
+3′-sulfo-Le^x	1.95	44 240	98.1 (95.6)	2.5 (2.3)	5.4 (25.0)	40 985	20.5	25.5
+4′-sulfo-Le^x	2.0	41 052	97.5 (94.7)	2.2 (2.1)	4.8 (24.2)	34 603	20.8	27.1

[a] All statistics are computed with a low-resolution cutoff of 10 Å. Values in parentheses are for the highest-resolution shell: for native data, 2.17−2.10 Å; for 3′-NeuAc-Le^x and 4′-sulfo-Le^x data, 2.07−2.00 Å; for 3′-sulfo-Le^x data, 2.02−1.95 Å. [b] $R_{sym} = \sum_h\sum_i[|I_i(h) - \langle I(h)\rangle|/\sum_h\sum_i I_i(h)]$, where $I_i(h)$ is the ith measurement and $\langle I(h)\rangle$ is the weighted mean of all measurements of $I(h)$. [c] Number of reflections in the working set (90% of total reflections; remaining 10% dedicated to test set). [d] $R_{cryst} = \sum_h||F(h)_{obs}|-|F(h)_{calc}||/\sum_h|F(h)_{obs}|$ for reflections in the working set. [e] $R_{free} = \sum_h||F(h)_{obs}|-|F(h)_{calc}||/\sum_h|F(h)_{obs}|$ for reflections in the test set.

Table 2: Model Geometry and Temperature Factors

crystal	unit cell[a]: *a* (Å)	*b* (Å)	*c* (Å)	*β* (deg)	total atoms	water atoms	rmsd from ideal values: bond length (Å)	bond angle (deg)	temperature factors: bond/angle-related rmsd (Å^2)	average/protomer: 1 (Å)	2 (Å)	3 (Å)
K3	79.7	84.9	98.7	105.3	3932	446	0.008	1.3	3.1/4.7	22.3	33.5	27.7
+3′-NeuAc-Le^x	79.1	85.0	98.8	107.1	4127	464	0.007	1.2	2.8/4.3	18.4	23.1	24.3
+3′-sulfo-Le^x	79.1	84.9	97.2	106.6	4042	462	0.007	1.2	3.1/4.7	19.1	25.7	27.4
+4′-sulfo-Le^x	79.1	85.0	97.5	106.3	4022	433	0.007	1.2	3.0/4.6	20.2	27.5	25.0

[a] From postrefinement in SCALEPACK (Otwinowski, 1993)

temperature factor refinement, and model building. Non-crystallographic symmetry restraints were not imposed at any point during refinement. Resolution-dependent weighting was also applied as $1/[1 - 2(1/2d - 1/6)]^2$, where d is the Bragg spacing of the reflection. Analysis of the data revealed significant anisotropy, so an overall anisotropic temperature factor tensor was refined and applied as described (Weis & Drickamer, 1994). Regions where the electron density did not fit the model were omitted, and the remaining subjected to simulated annealing refinement at 1000 K. The model was then modified according to the resulting difference electron density (Hodel et al., 1992). The conformations of the bound oligosaccharides were also confirmed by this procedure. Statistics on refinement and model geometry are presented in Tables 1 and 2.

RESULTS AND DISCUSSION

Structure of the Unliganded K3 Mutant. The final model contains all 149 residues for each of the three protomers in the asymmetric unit. Electron density is present for all main chain atoms but is weak or absent for the following surface side chains: in protomer 1, Lys^{118}; in protomer 2, Asp^{200}; and in protomer 3, Lys^{123}, Glu^{142}, Lys^{152}, and Asp^{200}. All main chain torsion angles are within allowed regions of the Ramachandran plot, and model geometry and temperature factor statistics are summarized in Table 2. Coordinate error, as assessed by Luzzati analysis, is in the range of 0.20−0.25 Å (Luzzati, 1952). When the K3 trimer is superimposed on that of wild-type MBP-A, the rmsd for 447 α-carbon atoms is 0.35 Å.

The mutation of residues 211−213 to Lys-Lys-Lys introduces a localized change in the structure of MBP-A which greatly resembles the structure of the corresponding region of E-selectin (Figure 1). The side chain of Lys^{213} is packed over Phe^{156}, which is equivalent to the packing of Lys^{113} onto Trp^{50} of E-selectin. The side chains of Lys^{211} and Lys^{212}, which are nearly fully exposed to the solvent, are well ordered in copies 1 and 3 but are not visible beyond Cγ in copy 2. The main chain conformation of residues 211−213 in K3 is similar to that of unliganded E-selectin, and superimposing all Ca^{2+} ligands (Ca^{2+} site 2; Weis et al., 1991) common to E-selectin and K3 shows that the position of this loop with respect to the Ca^{2+} ligands is also very similar in the two proteins. This superposition (Figure 1) yields an rmsd of 0.25 Å for the Ca^{2+} and Ca^{2+} ligands (41 atoms). The same rmsd is obtained if the main chain atoms of Lys$^{211-213}$ are also included in the fitting (50 atoms total). Moreover, the positions of corresponding lysine side chains are similar, even though individual torsion angles differ. Thus, the framework of the ligand binding site in K3 closely mimics that of E-selectin.

Structure of the Complex Formed by 3′-NeuAc-Le^x and K3. 3′-NeuAc-Le^x at 100 mM was soaked into a crystal of K3, and the coordinates of unliganded K3 were refined against data measured from this crystal. Apart from the displacement of water molecules from the bound calcium ion and the protein surface, sugar binding does not perturb the structure of the protein significantly. Strong difference electron density at Ca^{2+} site 2 of protomer 1 clearly defined the conformation of bound 3′-NeuAc-Le^x. As previously observed for wild-type and mutant MBP-As in the same crystal form, the electron density of protomers 2 and 3 is weaker than that defining protomer 1, particularly for the sugar ligands (Kolatkar & Weis, 1996). This effect is reflected in the refined temperature factors (Table 2) and most likely arises from differences in lattice packing for the three protomers. Simulated annealing omit electron density indicates that the conformation of the Le^x core of the sugar and the positions of the Lys side chains in protomer 1 are clearly defined in all K3-oligosaccharide complexes (Figure 2), but the electron density is too weak to permit building of a complete model of the oligosaccharide bound to the other two protomers. Nonetheless, the electron density present in the other two copies is consistent with the

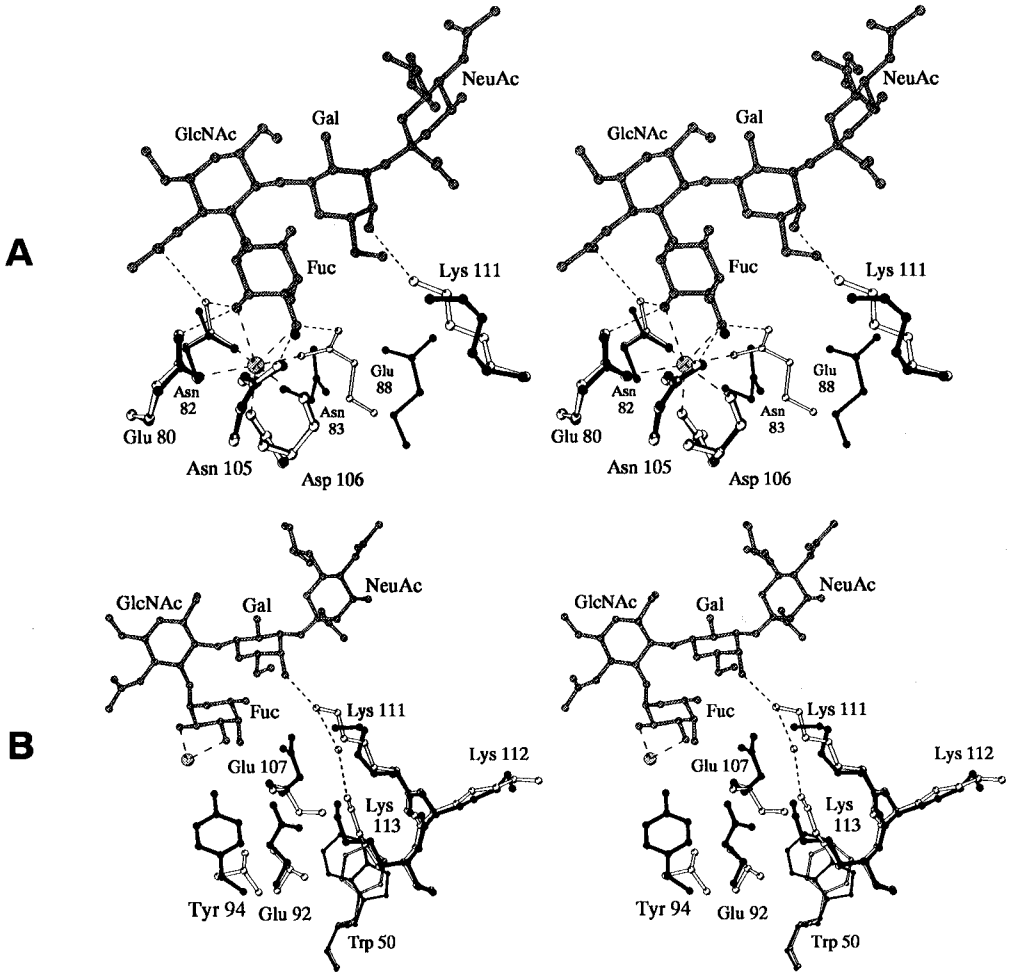

FIGURE 1: Stereoviews of unliganded E-selectin superimposed onto the complex of 3′-NeuAc-Le^x and K3. Note that the structure of K3 does not change significantly upon binding 3′-NeuAc-Le^x, and a virtually identical figure is obtained when the coordinates of unliganded K3 are used in the superposition. Ca^{2+} ligands in E-selectin (Glu^{80}, Asn^{82}, Asn^{105}, and Asp^{106}) and the corresponding residues in protomer 1 of K3 (Glu^{185}, Asn^{187}, Asn^{205}, and Asp^{206}) were used for the superposition. The protein atoms of K3 are drawn in white, E-selectin in black, and 3′-NeuAc-Le^x in gray. Hydrogen bonds are indicated by short dashed lines and coordination bonds by long dashed lines. (A) The ligands for Ca^{2+} in both E-selectin and K3 are shown. Whereas the four ligands used in the superposition fit closely, several other ligands adopt different conformations in E-selectin and K3. Glu^{88} from E-selectin differs from Glu^{193} of K3, and Asn^{83} of E-selectin differs from Asp^{188} of K3 (not shown). Also shown is a water molecule that forms a hydrogen bond with Asn^{83} and a coordination bond to Ca^{2+} in E-selectin. (B) Residues that are postulated to interact with the bound oligosaccharide in E-selectin (Glu^{92}, Tyr^{94}, Glu^{107}, Lys^{111}, Lys^{113}, as well as Lys^{112}) are shown along with corresponding residues from K3 (Thr^{197}, Val^{199}, Ile^{207}, Lys^{211}, Lys^{213}, as well as Lys^{212}). A water molecule that forms hydrogen bonds to both Lys^{211} and Lys^{213} of K3 is also shown, as are Trp^{50} of E-selectin and Phe^{156} of K3, which are packed under Lys^{113} of E-selectin and Lys^{213} of K3, respectively. Figures 1 and 3 were prepared using Molscript (Kraulis, 1991).

conformation of the oligosaccharide modeled for the sugar bound to protomer 1. No direct contacts are formed between the bound oligosaccharides and neighboring protein molecules in the crystal lattice. However, several residues and solvent molecules that interact with the sugar ligands are well-ordered due to interactions with lattice neighbors, which may contribute to the superior electron density of the sugar bound to protomer 1. For all of the oligosaccharide complexes described here, only the complex for protomer 1 is analyzed and discussed in detail.

The Fuc residue of 3′-NeuAc-Le^x is a principal determinant of binding, forming six direct contacts with the protein (Figure 3, Table 3). Most notably, the 2- and 3-OH of Fuc form a network of coordination bonds with Ca^{2+} and cooperative hydrogen bonds with four Ca^{2+} ligands in a manner similar to that observed for α-Me-Fuc or *β*-Me-Fuc bound to rat liver MBP-C (Ng et al., 1996) or rat serum MBP-A (A. Kolatkar, S. Snyder, and W. Weis, unpublished observations). A subtle but significant difference is that the position of Fuc is rotated slightly from the position seen in MBP-C and MBP-A. If the Ca^{2+} and Ca^{2+} ligands of MBP-C in five different monosaccharide complexes are superimposed, the rings of Fuc and other monosaccharides can be aligned with additional rotations of 3−11°. If the same MBP-C residues are superimposed onto their counterparts in K3, an additional rotation of 24° is required to superimpose α-Me-Fuc onto the Fuc residue of 3′-NeuAc-Le^x. When it is compared to the monosaccharide−MBP-C complexes, there is a slight increase in hydrogen bond distances and an increased asymmetry in the position of Fuc relative to the Ca^{2+} ligands, with Fuc tilted away from His^{189} and twisted slightly toward Asn^{205}.

Part of the rotation of Fuc in the 3′-NeuAc-Le^x−K3 complex relative to the position of Fuc bound to the MBPs may be due to the presence of the α(1−3)-linked GlcNAc residue. GlcNAc is sandwiched between Fuc and His^{189} (Figure 3) and makes four direct contacts and one water-mediated contact with the protein. The exocyclic acetamido O7 of GlcNAc accepts hydrogen bonds from Nδ2 of Asn^{187} and from a water molecule which in turn forms a hydrogen

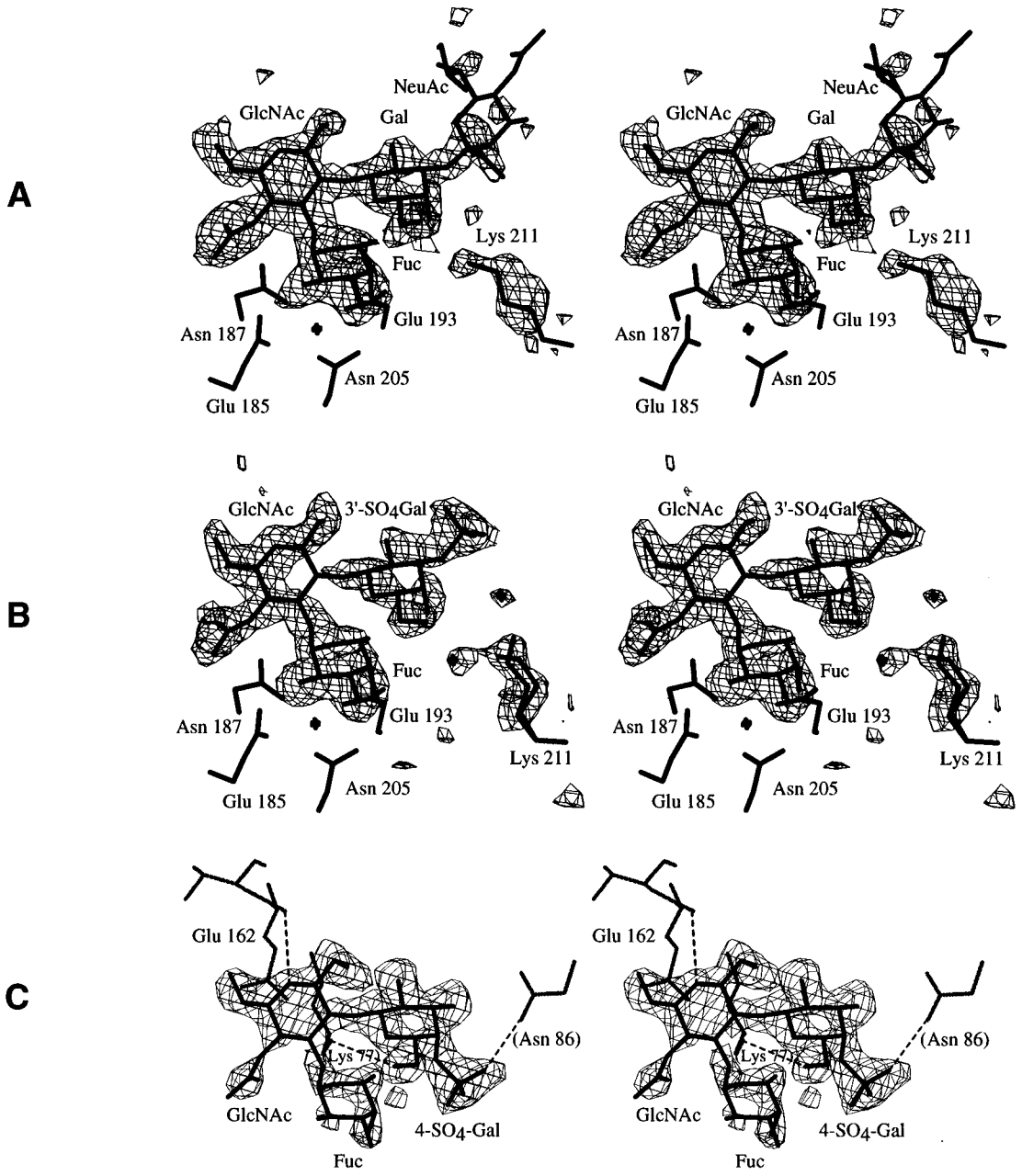

FIGURE 2: Stereoviews of simulated annealing (SA) omit electron density. Portions of the model were omitted for SA refinement and subsequent map calculations. $|F_o| - |F_c|$ maps were each contoured at 2.4σ above the mean. (A) 3′-NeuAc-Le^x bound to protomer 1 of K3 and all atoms past the Cβ atom of Lys^{211} were omitted. (B) 3′-sulfo-Le^x bound to protomer 1 of K3 and all atoms past the Cβ atom of Lys^{211} were omitted. (C) 4′-Sulfo-Le^x bound at an artifactual crystal lattice contact was omitted. Parentheses denote a residue related by crystallographic symmetry.

bond with the main chain carbonyl oxygen of residue 184. Both of these interactions are likely to occur in the selectins. In addition, the GlcNAc 6-OH forms a hydrogen bond with His^{189} in K3, and the GlcNAc C2 and C4 atoms contact Nϵ2 and Cϵ1 of this same His. The interactions with His^{189} would not be present in a complex of E-selectin with 3′-NeuAc-Le^x, since the loop in E-selectin that contains the corresponding residue is displaced away from the binding site [Figure 2c of Graves et al. (1994)].

The Gal residue of the oligosaccharide ligand is β(1−4)-linked to GlcNAc and is also packed against Fuc, completing the well-packed Le^x core. Gal makes two interactions with the protein. The 4-OH accepts a hydrogen bond from Lys^{211}, and the 6-OH forms a hydrogen bond with a water molecule that in turn forms hydrogen bonds with three protein atoms, Lys^{211} Nζ, Glu^{193} Oϵ2, and Ser^{208} N.

The NeuAc residue makes few interactions with the rest of the sugar and does not contact the protein. The electron density of the terminal α(2−3)-linked NeuAc residue is weaker than that of the rest of the oligosaccharide. However, the carboxylate moiety is well-defined and is 4.5 Å from the nearest protein atom, Lys^{211} Nζ. In contrast, the *N*-acetyl and glycerol substituents of NeuAc are not defined by electron density. These groups have been modeled in the conformations seen in crystal structures and NMR studies of NeuAc and oligosaccharides containing NeuAc [e.g., Flippen (1973), O'Connell (1973), Wright (1992), Acquotti et al. (1990), and Mukhopadhyay and Bush (1994)].

The only interactions between the newly introduced Lys residues and 3′-NeuAc-Le^x are the hydrogen bond formed between Lys^{211} Nζ and the Gal 4-OH and the water-mediated hydrogen bond formed between the same Lys Nζ and Gal

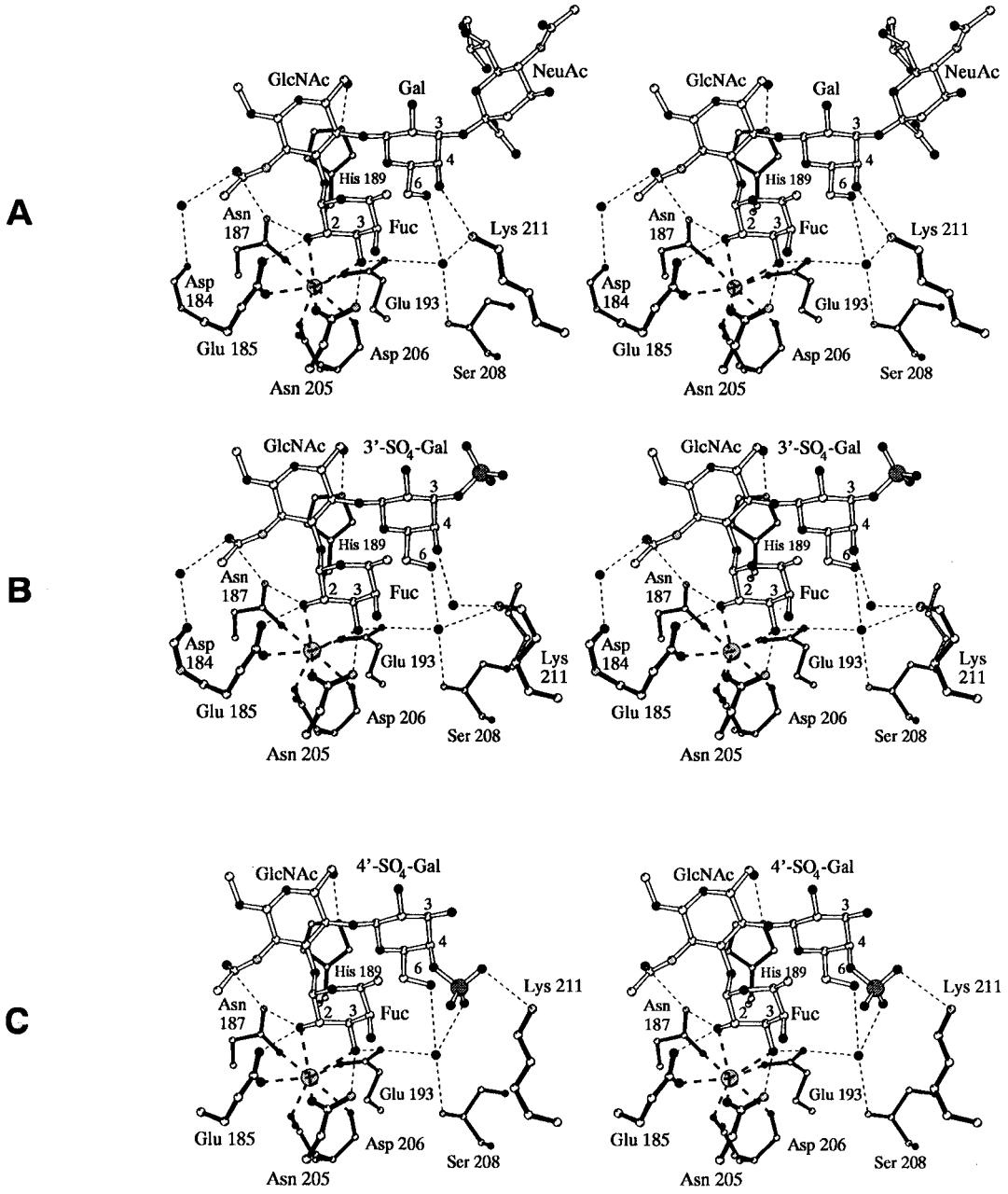

FIGURE 3: Stereoviews of the oligosaccharide−protein complexes. Bonds between protein atoms are drawn in black and bonds between sugar atoms in white. Carbon atoms are colored white, nitrogen atoms gray, and oxygen atoms black. Ca^{2+} and sulfur are shown as larger light and dark gray spheres, respectively. Hydrogen bonds between sugar and protein are indicated by short dashed lines and coordination bonds with Ca^{2+} by long dashed lines. For 3′-sulfo-Le^x, one of the alternate conformations of Lys^{211} is drawn with gray bonds: (A) 3′-NeuAc-Le^x, (B) 3′-sulfo-Le^x, and (C) 4′-sulfo-Le^x.

6-OH. Lys^{212} extends away from the bound sugar and out into solution. Lys^{213} extends toward the sugar but is over 9 Å from the nearest sugar atom. This residue forms a water-mediated hydrogen bond with Lys^{211}, which may stabilize the conformation of Lys^{211} that is needed for interaction with 3′-NeuAc-Le^x.

Correlations between the 3′-NeuAc-Le^x−K3 Structure and Results from Mutagenesis and Chemical Modification Studies on the Selectins. The relatively large number of interactions formed between the Fuc residue of 3′-NeuAc-Le^x and K3 is consistent both with binding studies indicating that Fuc is an essential component of selectin ligands and with mutagenesis experiments suggesting an important role for Ca^{2+} and its protein ligands (Berg et al., 1991; Tyrrell et al., 1991; Graves et al., 1994). The Fuc 2-, 3-, and 4-OH are essential for binding to E- and L-selectins (Brandley et al., 1993; Ramphal et al., 1994). In the K3 complex, the 2- and 3-OH form coordination bonds with Ca^{2+} and cooperative hydrogen bonds with the Ca^{2+} ligands in a manner believed to be common to C-type lectins which bind to sugars containing equatorial vicinal hydroxyl groups in the same stereochemistry (Ng et al., 1996). The importance of the 4-OH is also consistent with the observed mode of binding, even though it does not interact with K3. Superposition of E-selectin onto the 3′-NeuAc-Le^x−K3 complex reveals that both Tyr^{94} and Glu^{92}, which site-directed mutagenesis studies have identified as important for ligand binding (Hollenbaugh et al., 1993; Bajorath et al., 1994; Graves et al., 1994; Kogan et al., 1995), are poised to form hydrogen bonds with Fuc 4-OH (Figure 1B). The absence of these interactions in K3 may reduce the affinity of K3 for the oligosaccharide but probably does not affect the conformation of the bound oligosaccharide.

Table 3: Sugar-Protein Interactions

(A) Interactions Common to All Complexes

sugar atom	protein atom/Ca^{2+}	distances ± SD[a] (Å)	type of interaction
Fuc O2	Ca^{2+}	2.57 ± 0.04	coordination bond
O2	Glu^{185} Oϵ2	2.70 ± 0.08	hydrogen bond
O2	Asn^{187} Oδ1	3.03 ± 0.08	hydrogen bond
O3	Ca^{2+}	2.75 ± 0.03	coordination bond
O3	Glu^{193} Oϵ2	2.60 ± 0.02	hydrogen bond
O3	Asn^{205} Oδ1	3.33 ± 0.04	hydrogen bond
GlcNAc C2	His^{189} Cϵ1	4.03 ± 0.06	van der Waals
C4	His^{189} Nϵ2	3.71 ± 0.08	van der Waals
O6	His^{189} Nϵ2	2.93 ± 0.05	hydrogen bond
O7	Asn^{187} Nδ2	3.07 ± 0.06	hydrogen bond
Gal O6	Glu^{193} Oϵ2	3.18/2.74 ± 0.16/0.03	water-mediated
O6	Ser^{208} N	3.18/2.99 ± 0.16/0.06	water-mediated

(B) Interactions Specific to Individual Complexes

complex	sugar atom	protein atom	distances[a] (Å)	type of interaction
3′-NeuAc-Le^x	GlcNAc O7	Asp^{184} O	3.1/3.0	water-mediated
	Gal O4	Lys^{211} Nζ	3.0	hydrogen bond
	Gal O6	Lys^{211} Nζ	3.3/2.9	water-mediated
3′-sulfo-Le^x	GlcNAc O7	Asp^{184} O	3.1/2.8	water-mediated
	Gal O6	Lys^{211} Nζ	3.0/3.2	water-mediated
4′-sulfo-Le^x 1	Gal OS	Lys^{211} Nζ	3.5	salt bridge
	Gal OS	Glu^{193} Oϵ2	3.3/2.7	water-mediated
	Gal OS	Ser^{208} N	3.3/3.1	water-mediated
4′-sulfo-Le^x 2[b]	GlcNAc O5	Glu^{162} O	3.4	hydrogen bond
	Gal O6	(Lys^{77} Nζ)[b]	3.3	hydrogen bond
	Gal OS	(Asn^{86} Nδ2)[b]	3.0	hydrogen bond

[a] Distances were measured from complexes formed with protomer 1, because the electron density was better defined at this copy. For common interactions, the mean and standard deviation were calculated from three distances, one from each sugar complex. For water-mediated contacts, the first distance is between the sugar atom and water, and the second distance is between the protein atom and water. [b] Second site formed by crystal lattice packing. Parentheses denote atoms related by crystallographic symmetry.

Superposition of E-selectin and K3 reveals another difference that may give rise to a different mode of binding to 3′-NeuAc-Le^x by the selectins. Glu^{193} in K3 and wild-type MBP structures has a different conformation than that of the equivalent residue, Glu^{88}, in E-selectin. In the MBPs, this glutamate is a ligand of the site 2 Ca^{2+}. In E-selectin, Glu^{88} is displaced relative to MBP-A Glu^{193}, and instead, a water molecule held in position by Asn^{83} serves as the equivalent Ca^{2+} ligand [Figure 1A; Figure 2C of Graves et al. (1994); Figure 2 of Weis (1994)]. In E-selectin, the 3-OH of Fuc may form a hydrogen bond with the water molecule, or the 3-OH may displace the water molecule in a manner analogous to the displacement of water molecules upon monosaccharide binding to MBP-C (Ng et al., 1996). In the first case, the bound water molecule simply replaces the carboxylate oxygen atom of Glu^{193} in the current structure, and the mode of sugar binding seen in the K3 complex would be essentially preserved. In the alternative scheme, the position of Fuc would be rotated significantly from the position observed in the K3 complex, causing the rest of the oligosaccharide to swing away from the Lys residues at positions 111−113 of the selectins. This scenario seems less likely, because it would place the bound oligosaccharide too far from the Lys residues as well as from Tyr^{94} and Glu^{92} for these residues to interact with the sugar.

Binding studies are also consistent with the observation of interactions between Lys^{211} and the bound oligosaccharide. The hydrogen bond between Gal 4-OH and Lys^{211} Nζ, and the water-mediated hydrogen bond between Gal 6-OH and Lys^{211} Nζ, both help to explain the observation that conversion of either 4-OH or 6-OH to H reduces binding affinity (Stahl et al., 1994). The importance of these interactions is also reflected in decreased or abolished binding of 3′-NeuAc-Le^x to selectins when Lys^{111} is changed to Ala (Erbe et al., 1992, 1993; Hollenbaugh et al., 1993; Graves et al., 1994) and a chemical modification study showing that the Lys^{111} → Cys mutant of P-selectin binds HL-60 cells only after treatment with aziridine or nipsylcysteamine (Hollenbaugh et al., 1995).

Like Lys^{111}, Lys^{112} and Lys^{113} are conserved in the selectins. The equivalent residues of K3, Lys^{212} and Lys^{213}, do not interact directly with 3′-NeuAc-Le^x. The role of Lys^{112} has not been examined by mutagenesis, but mutation of Lys^{113} to Ala in E- and P-selectins results in the loss of binding to 3′-NeuAc-Le^x glycolipids, HL-60 cells, and neutrophils (Erbe et al., 1992, 1993; Hollenbaugh et al., 1993; Graves et al., 1994; Kogan et al., 1995; Revelle et al., 1996). The loss-of-function phenotype of the Lys^{113} → Ala mutants, in conjunction with modeling studies, prompted the prediction that the positive charge of Lys^{113} might directly interact with the negatively charged carboxylate of 3′-NeuAc-Le^x. However, subsequent studies demonstrate that a positively charged residue at this position is not necessary, as replacement of Lys with Gln or Glu allows binding to HL-60 cells and 3′-NeuAc-Le^x glycolipids (Kogan et al., 1995; Revelle et al., 1996). Moreover, replacement of Lys^{113} with Arg in either E-selectin (Kogan et al., 1995) or P-selectin (Bajorath et al., 1994) eliminates oligosaccharide binding. Therefore, instead of a direct charge−charge interaction with the sugar, data from both crystallography and mutagenesis suggest an indirect role for Lys^{113} in selectin−oligosaccharide interactions. In the unliganded E-selectin structure, Lys^{113} is packed over Trp^{50}, and in K3, Lys^{213} is packed over Phe^{156}, suggesting that the aliphatic portion of the Lys side chain helps to stabilize the structure. Modeling suggests that similar packing interactions can be formed by Glu or Gln at this position, but the bulkier Arg side chain would not fit in E-selectin without rearrangement of other residues. Lys^{113} Nζ in E-selectin forms a salt link with Glu^{92}, an interaction missing in K3, where Glu^{92} is replaced by Thr^{197}. Instead, Lys^{213} Nζ of K3 forms a hydrogen bond with a water molecule, which is in turn hydrogen bonded to Lys^{211}. Thus, in both cases, Lys^{113} may help position another residue which directly interacts with the sugar.

The most surprising aspect of the structure of the 3′-NeuAc-Le^x−K3 complex structure is that the NeuAc residue, and in particular the carboxylate moiety, does not directly contact the protein. Addition of the 3′-NeuAc residue to Le^x or Le^a oligosaccharides dramatically increases affinity for the selectins, and the binding of chemically modified sugars indicates that the carboxylate group is an important determinant of binding (Tyrrell et al., 1991; Brandley et al., 1993; Nelson et al., 1993). The lack of a direct interaction between the 3′-NeuAc residue and K3 may indicate that the orientation of the ligand observed in the crystal structure differs from the natural mode of binding to the selectins. The carboxylate moiety is fairly close to Lys^{211} (4.5 Å), and a different χ_4 rotamer would bring Lys^{211} Nζ close enough to form a salt bridge. Thus, it is possible that a slight difference in the conformation of the corresponding Lys residue in the selectins or a small displacement of the sugar would allow the formation of a salt bridge. Alternatively, the carboxylate moiety might affect binding energetics

Table 4: Torsion Angles of Oligosaccharides[a]

(A) K3 Complexes

	3′-NeuAc-Le^x φ/ψ	3′-sulfo-Le^x φ/ψ	4′-sulfo-Le^x (Ca^{2+} 2 site) φ/ψ	4′-sulfo-Le^x (lattice contact site) φ/ψ
NeuAc−Gal	−68/102			
Gal−GlcNAc	−74/−105	−77/−104	−79/−102	−73/−103
Fuc−GlcNAc	−68/138	−68/134	−67/140	−66/139

(B) Previous Studies

	NMR free[b] φ/ψ	NMR-bound 1[b] φ/ψ	NMR-bound 2[b] φ/ψ	Le^x X-ray[c] (copy 1) φ/ψ	Le^x X-ray[c] (copy 2) φ/ψ
NeuAc−Gal	163/63	−79/127	−76/126		
Gal−GlcNAc	−66/−112	−65/−113	−81/−108	−80/−105	−71/−108
Fuc−GlcNAc	−72/145	−72/145	−82/146	−73/139	−77/139

[a] Torsion angles are defined as follows: φ for NeuAc−Gal, $C1_{NeuAc}-C2_{NeuAc}-O_{link}-C3_{Gal}$; φ for Gal−GlcNAc, $O5_{Gal}-C1_{Gal}-O_{link}-C4_{GlcNAc}$; φ for Fuc−GlcNac, $O5_{Fuc}-C1_{Fuc}-O_{link}-C3_{GlcNAc}$; ψ for NeuAc−Gal, $C2_{NeuAc}-O_{link}-C3_{Gal}-C4_{Gal;}$ ψ for Gal−GlcNAc, $C2_{Gal}-O_{link}-C4_{GlcNAc}-C5_{GlcNAc}$; and ψ for Fuc−GlcNAc, $C2_{Fuc}-O_{link}-C3_{GlcNAc}-C4_{GlcNAc}$. [b] NMR free torsion angles are from the GESA-A model of Ichikawa et al. (1992) and are similar to those reported from other NMR and molecular mechanics studies (Mukhopadhyay et al., 1994; Rutherford et al., 1994). NMR-bound 1 angles are from Figure 3 of Cooke et al. (1994) and the GESA-C model of Ichikawa et al. (1992). NMR-bound 2 torsion angles are from Figure 3 of Scheffler et al. (1995). NMR torsion angles in published reports were defined with respect to hydrogen atoms. These angles were converted to the crystallographic convention by assuming that using an hydrogen atom instead of either an oxygen or carbon atom as a reference alters the torsion angle by ±120°. [c] From the two copies in the asymmetric unit of the Le^x crystal structure (Perez et al., 1996); similar values were reported for an isomorphous crystal form solved at lower resolution (Yvelin et al., 1996).

indirectly, possibly through subtle changes in water or oligosaccharide structure, or long range electrostatic interactions with the protein. It is important to note that the complex formed between 3′-NeuAc-Le^x and K3 argues against previous proposals that Lys^{213} directly interacts with the carboxylate group (Erbe et al., 1992; Bajorath et al., 1994; Cooke et al., 1994), because the shortest distance between Lys^{213} and the sugar is over 9 Å. Direct interaction between the sugar and Lys^{213} would require a very different mode of binding, which seems unlikely.

The lack of interactions between K3 and the glycerol and *N*-acetyl substituents of NeuAc is also consistent with studies which show that modifications of these groups do not reduce binding affinity to the selectins significantly when presented on immobilized glycolipids (Brandley et al., 1993). This differs from another study which indicates a modest reduction of binding affinity of E-selectin for soluble oligosaccharides containing modified NeuAc moieties (Nelson et al., 1993).

Structures of the Complexes Formed by 3′- and 4′-Sulfo-Le^x and the K3 Mutant. Sulfated oligosaccharides have been shown to bind to the selectins with affinities comparable to that of 3′-NeuAc-Le^x (Brandley et al., 1993; Yuen et al., 1994). 3′-Sulfo- and 4′-sulfo-Le^x were soaked into crystals of unliganded K3, and data were measured to 1.95 and 2.0 Å, respectively (Table 1). Difference electron density near Ca^{2+} site 2 of protomer 1 clearly showed the conformations of bound oligosaccharides before models for the sugars were refined against the data. As discussed above, the electron density for the corresponding regions of protomers 2 and 3 is consistent with similar conformations for the bound oligosaccharides but is too weak to allow modeling of complete oligosaccharides.

The conformation of the Le^x portion of the sulfated sugars is nearly identical to that of 3′-NeuAc-Le^x, and the interactions that the Fuc and GlcNAc residues form with the protein are also the same (Table 3, Figure 3). In the 3′-sulfo-Le^x complex, electron density maps and refined temperature factors indicate that the Lys^{211} side chain exists in two conformations (Figures 2B and 3B). In one of the conformations, Nζ forms hydrogen bonds with two water molecules which in turn are linked to the Gal 4- and 6-OH (Figure 3B). In the case of 4′-sulfo-Le^x, the sulfate moiety forms a salt bridge with Lys^{211}.

Binding studies suggest that glycolipids containing 3′-sulfo-Le^x and 3′-sulfo-Le^a bind to E- and L-selectin with higher affinity than nonsulfated analogs (Brandley et al., 1993; Yuen et al., 1994). It is therefore surprising that the sulfate moiety of 3′-sulfo-Le^x does not contact the protein directly (Figures 2B and 3B). As discussed for the carboxylate moiety in the 3′-NeuAc-Le^x complex, the sulfate group may exert indirect effects on binding energetics that are not apparent in the crystal structure.

Structures of the Bound Oligosaccharides. The structures of sulfo- and NeuAc-Le^x oligosaccharides bound to K3 are the first structures of substituted Le^x-type oligosaccharides determined by crystallography. The structure of the Le^x core is very similar in each of the bound sugars (Figure 3, Table 4), even though each of these structures was built and refined independently. Moreover, although the structures were built without bias from previously published studies on the conformations of Le^x-type sugars, the final refined models are similar to the high-resolution crystal structure of a Le^x hydrate (Perez et al., 1996; Yvelin et al., 1996) and structures proposed from molecular mechanics calculations and NMR spectroscopy (Berg et al., 1991; Ball et al., 1992; Ichikawa et al., 1992; Kogelberg & Rutherford, 1994; Mukhopadhyay et al., 1994; Rutherford et al., 1994). Torsion angles for the glycosidic linkages are presented in Table 4. Most torsion angles are within 5−10° of those determined by crystallography or NMR and molecular mechanics calculations.

The largest difference between the crystal structure of 3′-NeuAc-Le^x complexed with K3 and the structures of the oligosaccharide derived from NMR and molecular mechanics is in the relative orientations of NeuAc and Gal. The positions of these residues are defined by clear electron density for the Gal−NeuAc linkage and the proximal portion of the NeuAc residue. The conformation is similar to one

of the low-energy conformations predicted by molecular mechanics calculations (Ichikawa et al., 1992; Mukhopadhyay et al., 1994), but ψ differs from the calculated value by about 25° (Table 4). However, the energy wells for torsion angles in this linkage are quite broad, so the conformation seen in the crystal structure is clearly in the same energy well as the one proposed from molecular mechanics calculations (Mukhopadhyay & Bush, 1994; Rutherford et al., 1994).

The agreement between the structures of 3′-NeuAc-Le^x bound to K3 and those obtained by molecular mechanics calculations and NMR measurements for 3′-NeuAc-Le^x bound to E-selectin (Cooke et al., 1994; Scheffler et al., 1995) supports the conclusion that the bound conformation differs from that most likely populated by the sugar when it is free in solution (Ichikawa et al., 1992; Mukhopadhyay et al., 1994; Rutherford et al., 1994). The torsion angles of the Gal−NeuAc linkage (Table 4) in the bound conformation position the NeuAc carboxylate on the face of the oligosaccharide adjacent to Lys^{211} of K3, whereas the free conformation of the sugar would place the carboxylate group on the opposite face of the oligosaccharide.

The structures of the sulfo-substituted oligosaccharides complexed with K3 also agree with predictions from other crystallographic, molecular mechanics, and NMR studies. The conformation of the Le^x core is not affected by the addition of either 3′- or 4′-sulfate groups. Similar observations have been made from molecular dynamics and NMR indicating that the addition of sulfate does not perturb the conformation of the Le^a core (Kogelberg & Rutherford, 1994). The geometry of the linkage between sulfate groups and Gal is also similar to that seen in small molecule crystal structures and calculations on sulfated galactosides (Kanters et al., 1991; Lamba et al., 1994). In both the 3′- and 4′-sulfo-Le^x complexes, the sulfate group is *trans* to the hydrogen atom of the ring carbon to which the sulfate group is directly bonded, a conformation which minimizes steric clash between adjacent sugar ring carbons and the bulky sulfate group.

Finally, an artifactual second binding site for 4′-sulfo-Le^x that is generated by a lattice contact reveals that the oligosaccharide is in the same conformation as when bound to Ca^{2+} site 2 (Figure 2C, Table 4). This binding site is not likely to be present in molecules in solution, as the sugar makes contact with two protein molecules brought together by crystal packing. Moreover, most of the direct and water-mediated contacts between the sugar and the protein are formed with the coiled-coil domain of K3, which is not present in the selectins. The similarity of the conformation of the Le^x core in the sugar bound at this site and in the sugars bound at the Ca^{2+} site confirms the prediction from molecular mechanics, NMR measurements, and small molecule crystal structures that the Le^x core adopts a similar conformation when bound to the protein and free in solution.

CONCLUSIONS

The study of gain-of-function mutations in MBP-A−E-selectin chimeras provides structural and mechanistic information on oligosaccharide binding that is complementary to the large body of information provided by loss-of-function mutants and chemical modification studies on the selectins and their ligands. The structures of several Le^x-type oligosaccharides bound to K3 reveal a common structure for the Le^x core and a common mode of binding regardless of the substituent at the 3- or 4-OH of Gal. The direct interactions of Fuc with Ca^{2+} and its ligands, and of the 4-OH of Gal with Lys^{211} provide a structural explanation for the loss-of-function phenotype arising from mutations in the Ca^{2+} ligands and Lys^{111} of E-selectin and for chemical modification studies that indicate the importance of Fuc and Gal in the oligosaccharide ligand. The reported loss of binding to 3′-NeuAc-Le^x and HL-60 cells upon mutating Lys^{113} to Ala appears to be an indirect effect, because the corresponding residue in K3, Lys^{213}, is over 9 Å from the bound oligosaccharide. Other residues identified by mutagenesis to be involved in carbohydrate binding are poised to interact with the bound oligosaccharide when the structure of unliganded E-selectin is superimposed onto the complex of 3′-NeuAc-Le^x and K3. Ongoing structural and mutagenesis studies on MBP−selectin chimeras should clarify the mechanisms used by selectins to bind to natural ligands and improve future attempts to design anti-inflammatory drugs targeted at disrupting selectin−carbohydrate interactions.

ACKNOWLEDGMENT

We thank Dr. K. Drickamer for providing protein, as well as comments on the manuscript. We also thank Dr. A. Kolatkar for helpful discussions. Work at SSRL was done under Proposal 3A06.

REFERENCES

Bajorath, J., Hollenbaugh, D., King, G., Harte, W., Eustice, D. C., Darveau, R. P., & Aruffo, A. (1994) *Biochemistry 33*, 1332−1339.

Ball, G. E., O'Neill, R. A., Schultz, J. E., Lowe, J. B., Weston, B. W., Nagy, J. O., Brown, E. G., Hobbs, C. J., & Bednarski, M. D. (1992) *J. Am. Chem. Soc. 114*, 5449−5451.

Berg, E. L., Robinson, M. K., Mansson, O., Butcher, E. C., & Magnani, J. L. (1991) *J. Biol. Chem. 266*, 14869−14872.

Blanck, O., Iobst, S. T., Gabel, C., & Drickamer, K. (1996) *J. Biol. Chem. 271*, 7289−7292.

Brandley, B. K., Kiso, M., Abbas, S., Nikrad, P., Srivasatava, O., Foxall, C., Oda, Y., & Hasegawa, A. (1993) *Glycobiology 3*, 633−639.

Brünger, A. T. (1992a) *Nature 355*, 472−475.

Brünger, A. T. (1992b) *X-PLOR manual, version 3.1*, Yale University Press, New Haven, CT.

Collaborative Computational Project No. 4 (1994) *Acta Crystallogr. D 50*, 760−763.

Cooke, R. M., Hale, R. S., Lister, S. G., Shah, G., & Weir, M. P. (1994) *Biochemistry 33*, 10591−10596.

Erbe, D. V., Wolitzky, B. A., Presta, L. G., Norton, C. R., Ramos, R. J., Burns, D. K., Rumberger, J. M., Rao, B. N. N., Foxall, C., Brandley, B. K., & Lasky, L. A. (1992) *J. Cell Biol. 119*, 215−227.

Erbe, D. V., Watson, S. R., Presta, L. G., Wolitzky, B. A., Foxall, C., Brandley, B. K., & Lasky, L. A. (1993) *J. Cell Biol. 120*, 1227−1235.

Flippen, J. L. (1973) *Acta Crystallogr. B 29*, 1881−1886.

Graves, B. J., Crowther, R. L., Chandran, C., Rumberger, J. M., Li, S., Huang, K.-S., Presky, D. H., Familletti, P. C., Wolitzky, B. A., & Burns, D. K. (1994) *Nature 367*, 532−538.

Hodel, A., Kim, S.-H., & Brunger, A. T. (1992) *Acta Crystallogr. A 48*, 851−858.

Hollenbaugh, D., Bajorath, J., Stenkamp, R., & Aruffo, A. (1993) *Biochemistry 32*, 2960−2966.

Hollenbaugh, D., Aruffo, A., & Senter, P. D. (1995) *Biochemistry 34*, 5678−5684.

Ichikawa, Y., Lin, Y.-C., Dumas, D. P., Shen, G.-J., Garcia-Junceda, E., Williams, M. A., Bayer, R., Ketcham, C., Walker, L. E., Paulson, J. C., & Wong, C.-H. (1992) *J. Am. Chem. Soc. 114*, 9283−9298.

Iobst, S. T., & Drickamer, K. (1994) *J. Biol. Chem. 269*, 15512−15519.

Iobst, S. T., & Drickamer, K. (1996) *J. Biol. Chem. 271*, 6686−6693.

Iobst, S. T., Wormald, M. R., Weis, W. I., Dwek, R. A., & Drickamer, K. (1994) *J. Biol. Chem. 269*, 15505−15511.

Jones, T. A., Zou, J.-Y., Cowan, S. W., & Kjeldgaard, M. (1991) *Acta Crystallogr. A 47*, 110−119.

Kanters, J. A., van Dijk, B., & Kroon, J. (1991) *Carbohydr. Res. 212*, 1−11.

Kogan, T. P., Revelle, B. M., Tapp, S., Scott, D., & Beck, P. J. (1995) *J. Biol. Chem. 270*, 14047−14055.

Kogelberg, H., & Rutherford, T. J. (1994) *Glycobiology 4*, 49−57.

Kolatkar, A. R., & Weis, W. I. (1996) *J. Biol. Chem. 271*, 6679−6685.

Kraulis, P. J. (1991) *J. Appl. Crystallogr. 24*, 946−950.

Lamba, D., Glover, S., Mackie, W., Rashid, A., Sheldrick, B., & Perez, S. (1994) *Glycobiology 4*, 151−163.

Laskowski, R. A., MacArthur, M. W., Moss, D. S., & Thornton, J. M. (1993) *J. Appl. Crystallogr. 26*, 283−291.

Luzzati, V. (1952) *Acta Crystallogr. 5*, 802−810.

McEver, R. P. (1994) *Curr. Opin. Immunol. 6*, 75−84.

Mukhopadhyay, C., & Bush, C. A. (1994) *Biopolymers 34*, 11−20.

Mukhopadhyay, C., Miller, K. E., & Bush, C. A. (1994) *Biopolymers 34*, 21−29.

Nelson, R. M., Dolich, S., Aruffo, A., Cecconi, O., & Bevilacqua, M. P. (1993) *J. Clin. Invest. 91*, 1157−1166.

Nelson, R. M., Venot, A., Bevilacqua, M. P., Linhardt, R. J., & Stamenkovic, I. (1995) *Annu. Rev. Cell Dev. Biol. 11*, 601−631.

Ng, K. K.-S., Drickamer, K., & Weis, W. I. (1996) *J. Biol. Chem. 271*, 663−674.

O'Connell, A. M. (1973) *Acta Crystallogr. B 29*, 2320−2328.

Otwinowski, Z. (1993) Oscillation reduction program, in *Data Collection and Processing* Sawyer, L., Isaacs, N., & Bailey, S., Eds.) pp 56−62, SERC Daresbury Laboratory, Daresbury, U.K.

Perez, S., Mouhous-Riou, N., Nifant'ev, N., Tsvetkov, Y. E., Bachet, B., & Imberty, A. (1996) *Glycobiology 6*, 537−542.

Ramphal, J. Y., Zheng, Z.-L., Perez, C., Walker, L. E., DeFrees, S. A., & Gaeta, F. C. A. (1994) *J. Med. Chem. 37*, 3459−3463.

Revelle, B. M., Scott, D., Kogan, T. P., Zheng, J., & Beck, P. J. (1996) *J. Biol. Chem. 271*, 4289−4297.

Rutherford, T. J., Spackman, D. G., Simpson, P. J., & Homans, S. W. (1994) *Glycobiology 4*, 59−68.

Scheffler, K., Ernst, B., Katopodis, A., Magnani, J. L., Wang, W. T., Weisemann, R., & Peters, T. (1995) *Angew. Chem., Int. Ed. Engl. 34*, 1841−1844.

Stahl, W., Sprengard, U., Kretzschmar, G., & Kunz, H. (1994) *Angew. Chem. Int. Ed. Engl. 33*, 2096−2098.

Tyrrell, D., James, P., Rao, N., Foxall, C., Abbas, S., Dasgupta, F., Nashed, M., Hasegawa, A., Kiso, M., Asa, D., Kidd, J., & Brandley, B. K. (1991) *Proc. Natl. Acad. Sci. U.S.A. 88*, 10372−10376.

Varki, A. (1994) *Proc. Natl. Acad. Sci. U.S.A. 91*, 7390−7397.

Weis, W. I. (1994) *Structure 2*, 147−150.

Weis, W. I., & Drickamer, K. (1994) *Structure 2*, 1227−1240.

Weis, W. I., Crichlow, G. V., Murthy, H. M. K., Hendrickson, W. A., & Drickamer, K. (1991) *J. Biol. Chem. 266*, 20678−20686.

Wright, C. S. (1992) *J. Biol. Chem. 267*, 14345−14352.

Yuen, C.-T., Bezouska, K., O'Brien, J., Stoll, M., Lemoine, R., Lubineau, A., Kiso, M., Hasegawa, A., Bockovich, N. J., Nicolaou, K. C., & Feizi, T. (1994) *J. Biol. Chem. 269*, 1595−1598.

Yvelin, F., Zhang, Y.-M., Mallet, J.-M., Robert, F., Jeannin, Y., & Sinay, P. (1996) *Carbohydr. Lett. 1*, 475−482.

BI962564E